Adjacent asparagines in the NR2-subunit of the NMDA receptor channel control the voltage-dependent block by extracellular Mg^{2+}

Lonnie P. Wollmuth, Thomas Kuner* and Bert Sakmann

*Abteilung Zellphysiologie and *Abteilung Molekulare Neurobiologie, Max-Planck-Institut für medizinische Forschung, Jahnstrasse 29, D-69120 Heidelberg, Germany*

(Received 10 January 1997; accepted after revision 12 September 1997)

1. The voltage-dependent block of *N*-methyl-D-aspartate (NMDA) receptor channels by extracellular Mg^{2+} is a critical determinant of its contribution to CNS synaptic physiology. The function of the narrow constriction of the channel in determining the block was investigated by analysing the effects of a set of different amino acid substitutions at exposed residues positioned at or near this region. NMDA receptor channels, composed of wild-type and mutant NR1- and NR2A-subunits, were expressed in *Xenopus* oocytes or human embryonic kidney (HEK) 293 cells.

2. In wild-type channels, the voltage dependence (δ) of the block by Mg^{2+} was concentration dependent with values of δ of ~0·58 in 0·01 mM and ~0·82 in 0·07 mM and higher concentrations. Under biionic conditions with high extracellular Mg^{2+} and K^+ as the reference ion, Mg^{2+} weakly permeated the channel. Over intermediate potentials (~−60 to −10 mV), this weak permeability had no apparent effect on the block but at potentials negative to ~−60 mV, it attenuated the extent and voltage dependence of the block.

3. Substitutions of glycine, serine, glutamine or aspartate for the N-site asparagine in the NR1-subunit enhanced the extent of block over intermediate potentials but left the voltage dependence of the block unchanged indicating that structural determinants of the block remained. These same substitutions either attenuated or left unchanged the apparent Mg^{2+} permeability.

4. In channels containing substitutions of glycine, serine or glutamine for the N-site asparagine in the NR2A-subunit, the block by Mg^{2+} was reduced at negative potentials. Over intermediate potentials, the block was not strongly attenuated except for the glutamine substitution which reduced the voltage dependence of the block to ~0·57 in 0·7 mM Mg^{2+}.

5. Equivalent substitutions for the N + 1 site asparagine in the NR2A-subunit strongly attenuated the block over the entire voltage range. In 0·7 mM Mg^{2+}, the voltage dependence of the block was reduced to 0·50 (glycine), 0·53 (serine) and 0·46 (glutamine).

6. Channels containing substitutions of the N-site or N + 1 site asparagines in the NR2A-subunit showed an increased Mg^{2+} permeability suggesting that these adjacent asparagines form a barrier for inward Mg^{2+} flux. Changes in this barrier contribute, at least in part, to the mechanism underlying disruption of the block following substitution of these residues.

7. The adjacent NR2A-subunit asparagines are positioned at or near the narrow constriction of the channel. Pore size, however, did not determine how effectively Mg^{2+} blocks mutant channels.

8. It is concluded that, at the narrow constriction in the NMDA receptor channel, the adjacent NR2A-subunit asparagines, the N-site and N + 1 site, but not the N-site asparagine of the NR1-subunit, form a critical blocking site for extracellular Mg^{2+}. The contribution to the blocking site, in contrast to the prevailing view, is stronger for the N + 1 site than for the N-site asparagine. The block may involve binding of Mg^{2+} to these residues.

Many biological functions of the *N*-methyl-D-aspartate (NMDA) receptor are mediated by the flux of Ca^{2+} through its open channel (MacDermott, Mayer, Westbrook, Smith & Barker, 1986; Mayer & Miller, 1988; Bliss & Collingridge, 1993). The pore of NMDA receptor channels is blocked by extracellular Mg^{2+} preventing Ca^{2+} as well as monovalent cation influx (Nowak, Bregestovsky, Ascher, Herbet & Prochiantz, 1984; Mayer, Westbrook & Guthrie, 1984). The strong voltage dependence of this block, which is relieved with membrane depolarization, makes the Ca^{2+} signalling mediated by NMDA receptors conditional: Ca^{2+} influx occurs only with presynaptic release of glutamate and coincident post-synaptic depolarization (Bliss & Collingridge, 1993).

In physiological solutions, the voltage dependence of the block by extracellular Mg^{2+} gives an apparent site of interaction between 0·8 and 1 across the transmembrane electric field (Ascher & Nowak, 1988; Jahr & Stevens, 1990*a*). One interpretation of this is that a single Mg^{2+} ion blocks the channel almost entirely across the electric field. However, the voltage dependence of the block by intracellular Mg^{2+} argues against extracellular Mg^{2+} blocking so deep in the channel (Johnson & Ascher, 1990; Li-Smerin & Johnson, 1996). The strong voltage dependence could therefore reflect the combined electrical distances of multiple Mg^{2+} ions (or one Mg^{2+} ion and one or more $Ca^{2+}/K^{+}/Na^{+}$ ions) entering the pore in a multi-ion process (but see Zarei & Dani, 1994). Alternatively, it could arise by other mechanisms such as ion–ion interactions within the pore (Ruppersberg, von Kitzing & Schoepfer, 1994; Zarei & Dani, 1995). Given that the deepest blocking point for extracellular Mg^{2+} is probably at or near the narrowest part of the channel, defining the contribution to the block of residues forming this region is essential for the development of a molecular picture of the block.

Native NMDA receptor channels are heteromers composed of the constitutive NR1-subunit and one or more of four different NR2-subunits (A, B, C, D) (Sheng, Cummings, Roldan, Jan & Jan, 1994; for review, see Hollmann & Heinemann, 1994). Based on sequence alignment, asparagine (N) residues in the pore-lining M2 segment of the NR1- and NR2-subunits occupy an identical position (Fig. 1*A*), homologous to the functionally critical Q/R-site in α-amino-3-hydroxy-5-methylisoxazole-4-propionate (AMPA) receptors (Hollmann & Heinemann, 1994). For both subunits, the N-site asparagines are exposed at the tip of a loop formed by the M2 segment (Fig. 1*B*), but these N-site asparagines are otherwise neither structurally nor functionally equivalent (Burnashev *et al.* 1992; Wollmuth, Kuner, Seeburg & Sakmann, 1996; Kuner, Wollmuth, Karlin, Seeburg & Sakmann, 1996). The narrowest part of the channel, termed the narrow constriction or selectivity filter (Hille, 1992), is formed primarily by the NR1-subunit N-site asparagine and an asparagine adjacent to the NR2A-subunit N-site, the N + 1 site (Fig. 1*B*; Wollmuth *et al.* 1996). In this working model, the NR2A-subunit N-site asparagine is positioned on the extracellular side of the narrow constriction (Fig. 1*B*; Kuner *et al.* 1996).

We examined how substitutions of residues positioned at or near the narrow constriction and exposed to the channel lumen (Fig. 1) contribute to extracellular Mg^{2+} block. Our goals were threefold. First, to determine which residues positioned near this region contribute to the block. Substitutions of these residues can have profound effects on Ca^{2+} permeability (Burnashev *et al.* 1992) as well as single channel properties (e.g. Premkumar & Auerbach, 1996; Schneggenburger & Ascher, 1997). We therefore recorded the block in the absence of Ca^{2+} (EGTA externally) and examined multiple substitutions at a single site, anticipating that if a side chain contributes to the block, a side chain-dependent pattern of block should be observed. The second goal was to determine whether the size of the narrow constriction contributes to the block. The size of hydrated Mg^{2+}, at least 0·7 nm, is larger than the estimated 0·55 nm pore size of NMDA receptor channels (Villarroel, Burnashev & Sakmann, 1995; Zarei & Dani, 1995; Wollmuth *et al.* 1996), and Mg^{2+} block at the narrow constriction could arise by steric occlusion. Since the substitutions change the pore size to a known degree (Wollmuth *et al.* 1996; see Methods), the contribution of the size of this region to the block can be determined. Finally, we wanted to determine, at least in part, how residues positioned at the narrow constriction interact with Mg^{2+}. We report that substitutions of two adjacent asparagines in the NR2A-subunit, especially that of the N + 1 site asparagine, but not of the N-site asparagine in the NR1-subunit, strongly reduce the block. These effects show little dependence on pore size suggesting that the block does not arise by steric occlusion. The adjacent NR2A-subunit asparagines contribute to the block mechanism in part by forming a barrier for inward Mg^{2+} flux as well as to some other process, possibly binding of Mg^{2+}.

METHODS

Heterologous expression of NMDA receptor channels

All experiments were performed with previously described expression constructs for wild-type and mutant NMDA receptor subunits (Wollmuth *et al.* 1996). As described, NR1 mutants were co-expressed with wild-type NR2A or vice versa in *Xenopus* oocytes and human embryonic kidney 293 cells (HEK 293; reference no., CRL 1573). *Xenopus* oocytes were taken from frogs anaesthetized in an ice bath containing 0·3% MS-222 for 40 min. For ease of description, mutated positions are identified by defining the N-sites as position '0' (Fig. 1*A*; Kuner *et al.* 1996).

Solutions

Substitutions of residues positioned near the narrow constriction may change monovalent cation as well as Ca^{2+} permeability. To compare extracellular Mg^{2+} block in wild-type and mutant channels, we therefore used symmetrical $[K^{+}]$ on both sides of the membrane forcing the reversal potential to 0 mV and included an extracellular Ca^{2+} buffer. In all instances, the intracellular solution consisted of (mM): 100 KCl, 10 Hepes and 10 BAPTA; pH adjusted

to 7·2 with KOH. For the extracellular solutions, the 10 mM BAPTA was replaced by 8 mM EGTA and 2 mM EDTA (0 Mg^{2+} control solution) or 10 mM EGTA to which $MgCl_2$ was added to yield the free Mg^{2+} concentration indicated in the text. Free Mg^{2+} concentrations were determined from apparent affinity constants for EGTA, measured with the potentiometric method, with software kindly provided by R. Thieleczek (Moisescu & Thieleczek, 1978; Stephenson & Thieleczek, 1986). In all instances block was measured using whole-cell recordings of HEK 293 cells. Mg^{2+} influx was quantified using HEK 293 cells and oocyte outside-out patches. The high-K^+ solution used as a reference to quantify inward Mg^{2+} permeability consisted of (mM): 100 KCl and 10 Hepes; pH adjusted to 7·2 with KOH. For outside-out oocyte patches, the same solution contained 0·18 mM $CaCl_2$. The high-Mg^{2+} solution consisted of (mM): 78 $MgCl_2$, 2 $Mg(OH)_2$ and 10 Hepes, with the final pH 7·2. The Mg^{2+} salts were of ultrapure grade (Merck, Darmstadt, Germany).

Current recordings and data analysis

Currents were recorded at room temperature (19–23 °C) using an EPC-9 amplifier with PULSE software (HEKA electronics GmbH, Lambrecht, Germany), low-pass filtered at 500 Hz, and digitized at 2 kHz. Pipettes were pulled from borosilicate glass and had resistances of 0·8–3 MΩ when filled with the pipette solution and measured in the K^+ solution. To ensure that voltage drops due to series resistance were less than 2 mV, we often used series resistance compensation (70–85%) with a lag time of 100 μs. Extracellular solutions were applied using a Piezo-driven double-barrel application pipette with one barrel containing the extracellular solution plus 50 μM glycine and the other barrel the same solution but with added 200 μM glutamate. The NMDA receptor current was defined as the difference between current recorded in the presence and absence of glutamate. The liquid-junction potential between the 103·5 mM K^+ solution and the KCl pipette solution was −2 mV (pipette negative). The 80 mM Mg^{2+} solution generated a junction

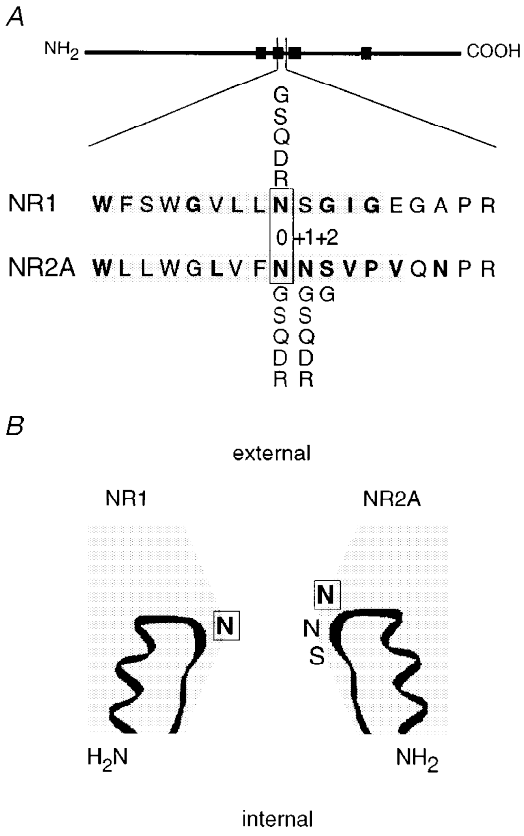

Figure 1. Amino acid sequence of the wild-type NR1 and NR2A M2-loop segments

A, schematic drawing of the NMDA receptor subunits with the four hydrophobic segments (M1 to M4) indicated as filled boxes and the enlarged region showing a sequence alignment of amino acid residues forming the core region of the loop; this core region includes residues from the M2 segment (shaded) and the short linker connecting the M2 and M3 segments. The N-site is designated position '0' with positions on the C-terminal side given a positive number. In the mature protein, the N-site asparagines correspond to position 598 (NR1) and 595 (NR2A). Residues that are exposed to the lumen of the channel are emboldened (Kuner *et al.* 1996). Five amino acids, glycine (G), serine (S), glutamine (Q), aspartate (D), and arginine (R), were substituted at positions NR1(N0), NR2A(N0) and NR2A(N + 1), whereas at the NR2A(S + 2) position, only glycine was substituted. *B*, positioning of exposed and polar residues near the narrow constriction. The two homologous asparagines (position 0; emboldened and boxed) are positioned in a staggered fashion with the N-site in the NR2A-subunit being more external than the NR2A-subunit N + 1 site and NR1-subunit N-site.

potential between the ground electrode and the high-KCl solution of −10·2 mV (ground electrode, 0 mV). All curve fitting was done using Igor Pro (WaveMetrics, Inc., Lake Oswego, OR, USA). Results are reported in the text as means ± S.E.M. and shown graphically as means ± 2 S.E.M.

Mg^{2+} permeability. Two measures of Mg^{2+} permeability in NMDA receptor channels with K^+ as a reference were quantified: changes in zero-current (reversal) potentials and relative chord conductances. Changes in the reversal potential (ΔE_r) were used as an approximate index of the driving force for Mg^{2+} relative to that for K^+. They were determined by measuring the change of the reversal potential for glutamate-activated currents on replacing the 103·5 mM K^+, 0·18 mM Ca^{2+} solution (for HEK 293 cells the solution contained no added Ca^{2+}) with a similar solution except that the K^+ was replaced by 80 mM Mg^{2+} and there was no added Ca^{2+}. Relative chord conductances (G_{Mg}/G_K) were used as an approximate index of the rate at which channels carry inward Mg^{2+} relative to K^+. Current amplitudes were measured at −120 mV (high Mg^{2+}) or −40 mV (high K^+) and corrected for their respective reversal potentials. For mutant channels, both indexes of Mg^{2+} permeability were of limited quantitative value since they require the assumption that the substitutions have no effect on K^+ permeation, a situation that probably does not hold. We therefore refer to these parameters as apparent permeability.

Voltage-dependent block. To model the relative location of a blocking site for Mg^{2+}, we assumed that Mg^{2+} acts within the transmembrane electric field. With a Woodhull model (Woodhull, 1973), the current amplitude in the presence (I_B) and absence (I_0) of Mg^{2+} are related according to the relationship:

$$I_B = \frac{I_0}{1 + \dfrac{[Mg^{2+}]_o}{K_{0.5}(0\text{ mV})\exp\left(\dfrac{z\delta EF}{RT}\right)}}, \quad (1)$$

where $K_{0.5}(0\text{ mV})$ is the half-maximal block at 0 mV, δ is the portion of the membrane electric field sensed by the blocking site and z is the valence of the blocking ion. R, T and F have their normal thermodynamic meanings and the quantity RT/F was 25·4 mV (21 °C). To control for run-down and to increase the accuracy of the measurement of the block over the entire voltage

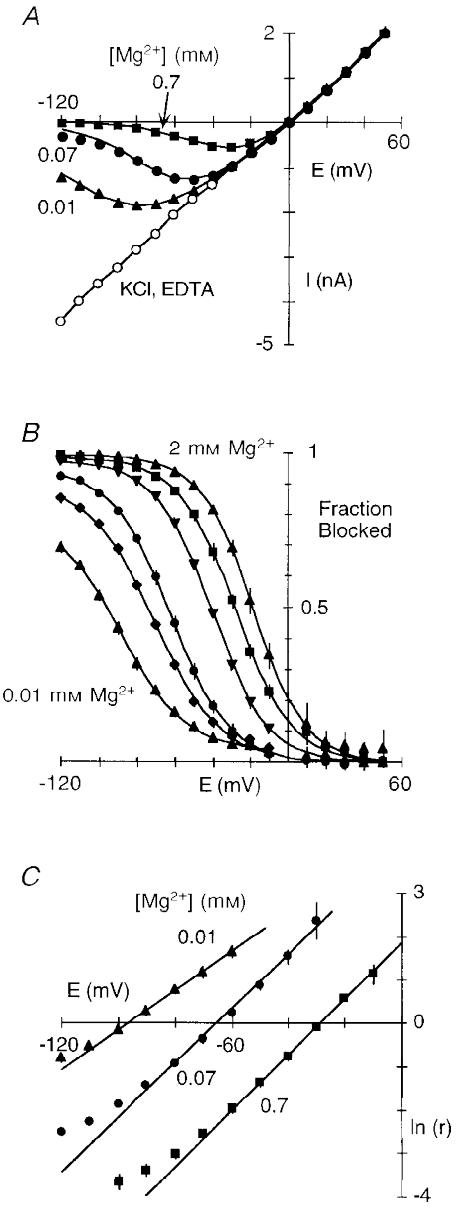

Figure 2. Voltage-dependent block of wild-type NR1–NR2A channels by extracellular Mg^{2+}

A, peak glutamate-activated currents plotted against membrane voltage in the absence (2 mM EDTA; KCl, EDTA) or presence of extracellular Mg^{2+} (0·01, 0·07 or 0·7 mM). Currents were generated by voltage steps, in 10 mV increments, and recorded in HEK 293 cells bathed in symmetrical [KCl] with 0 extracellular Ca^{2+}. The 0 Mg^{2+} recording is an average of the currents recorded before and after exposure to each Mg^{2+} concentration. The continuous lines through the points in Mg^{2+} are from eqn (1) with the parameters δ and $K_{0.5}(0\text{ mV})$ derived from eqn (2) (see *C*). Series resistance (R_s), 2·4 MΩ; R_s compensation, 80 %. *B*, mean fraction blocked ($1 - I_B/I_0$), where I_0 and I_B are the current amplitude in the absence and presence of different Mg^{2+} concentrations, respectively. In all instances, I_0 was the average of currents recorded before and after application of the individual Mg^{2+} concentration. Each point is shown as the mean ± 2 S.E.M., and corresponds to Mg^{2+} concentrations of 0·01 mM (triangles), 0·03 mM (diamonds), 0·07 mM (circles), 0·3 mM (inverted triangles), 0·7 mM (squares) and 2 mM (triangles). Continuous curves are fitted Boltzmann equations (eqn (3)). In all instances, a simple Boltzmann equation readily fitted the results except for the block by 0·01 mM where an additional component existed between −50 and −10 mV. *C*, mean $\ln(I_B/(I_0 - I_B))$ (eqn (2)), referred to as $\ln(r)$, plotted against voltage for three different Mg^{2+} concentrations. Lines were fitted over the apparent linear region from −100 to −60 mV (0·01 mM), −80 to −30 mV (0·07 mM) and −70 to −10 mV (0·7 mM). The analysis was restricted to $\ln(r)$ values less than 2·5 where the current amplitude was reduced by at least 10 %.

Table 1. Woodhull parameters for block of wild-type NR1-NR2A channels by extracellular Mg^{2+} in symmetrical [KCl]

$[Mg^{2+}]$ (mM)	δ	$K_{0.5}$(0 mV) (mM)	n
0·01	0·58 ± 0·02	0·8 ± 0·1	8
0·03	0·71 ± 0·01	2·0 ± 0·2	8
0·07	0·80 ± 0·01	4·3 ± 0·3	10
0·3	0·82 ± 0·01	4·5 ± 0·2	8
0·7	0·82 ± 0·01	4·4 ± 0·2	6
2	0·86 ± 0·01	7·2 ± 0·2	4

Solutions: intracellular (mM): 123·5 KCl, 10 Hepes, 10 Bapta; control (0 Mg^{2+}) extracellular (mM): 123·5 KCl, 10 Hepes, 8 EGTA, 2 EDTA. The composition of the test extracellular solution was the same except that EGTA replaced EDTA (10 mM EGTA) and $MgCl_2$ was added to obtain the free Mg^{2+} concentration. Parameters were derived by fitting the linear part of plots of $\ln(I_B/(I_0 - I_B))$ against voltage (eqn (2); see Fig. 2*C*). Fitted ranges were: −100 to −60 mV (0·01 mM), −90 to −40 mV (0·03 mM), −80 to −30 mV (0·07 mM), −70 to −10 mV (0·3 and 0·7 mM) and −60 to −10 mV (2 mM). Values are means ± S.E.M.

range, for each individual recording I_0 was an average of the current amplitude recorded before and after exposure to the Mg^{2+} concentration. We used two approaches to determine $K_{0.5}$(0 mV) and δ. First, a linear relationship was fitted to the linear region of $\ln(I_B/(I_0 - I_B))$, referred to as $\ln(r)$, plotted against voltage (DiFrancesco, 1982) where $\ln(I_B/(I_0 - I_B))$ is defined as:

$$\ln(I_B/(I_0 - I_B)) = z\delta FE/RT - \ln([Mg^{2+}]_o/K_{0.5}(0\text{ mV})). \quad (2)$$

The linear region was determined for average plots of $\ln(r)$ against voltage (using a maximal $\ln(r)$ of 2·5, i.e. where the block was at least 10%) and then the same voltage range was used to fit individual records. The second approach involved fitting the Boltzmann equation to the fraction blocked:

$$B(E) = \frac{B_{max}}{1 + \exp((E - E_{0.5})z\delta F/RT)}, \quad (3)$$

where B is the fraction blocked $(1 - I_B/I_0)$, B_{max} is the maximal fraction blocked, and $E_{0.5}$ is the voltage for half-maximal block. Assuming the blocking particle is impermeant:

$$K_{0.5}(0\text{ mV}) = [Mg^{2+}]_o \exp(E_{0.5}z\delta F/RT).$$

A more complex relationship arises when permeation is explicitly included in the derivation. When B_{max} is set equal to 1, this equation is identical to the Woodhull model (i.e. at extreme potentials all channels are blocked), and when fitted over the same voltage range as the $\ln(r)$ plots, it yielded indistinguishable parameters (data not shown). We therefore show values derived from this approach only when B_{max} was a free parameter.

The use of macroscopic currents to quantify the voltage dependence of the block assumes that the only effect Mg^{2+} has at the single channel level is to occlude the channel rather than, for example, to alter its open probability. For wild-type channels such an assumption seems warranted (Jahr & Stevens, 1990*b*). We assumed that the predominant effect the mutant channels have on the block process is to alter this occlusion process; detailed single channel studies will be necessary to verify this assumption. In addition, for wild-type, the macroscopic current–voltage relationship in the absence of Mg^{2+} was linear (see Fig. 2*A*) yet the underlying single channel amplitudes showed a significant inward rectification (Wollmuth, Kuner & Sakmann, 1998). The basis for this difference is an increase in open probability at positive potentials (Nowak & Wright, 1992). In the case of extracellular Mg^{2+}, this change in open probability presumably does not influence the block; at the concentrations of Mg^{2+} we tested (typically < 1 mM), the amplitudes of currents at positive potentials with or without Mg^{2+} present were identical in wild-type and all mutant channels indicating that block or potentiation at these potentials is negligible and that a constant number of channels are opened during the step.

Estimation of pore diameter. The size of the narrow constriction for wild-type and mutant channels was estimated using the relative permeability of differently sized organic cations (see Wollmuth *et al.* 1996). Usually, this estimate was based on at least four different organics. In some instances, we estimated pore diameter using two organics. Certain mutant channels were classified as having the same pore diameter as wild-type; alternatively, for substitutions which changed pore diameter we used the glycine (G) substitution of the same subunit (NR1(N0G) or NR2A(N + 1G)) and wild-type as calibration lines (see Fig. 8; Wollmuth *et al.* 1996).

RESULTS

Block of wild-type NR1–NR2A channels by extracellular Mg^{2+}

Figure 2*A* illustrates extracellular Mg^{2+} block of NR1–NR2A channels in symmetrical [KCl] with 0 extracellular Ca^{2+}. In the absence of Mg^{2+}, the current–voltage relationship was linear. When Mg^{2+} (0·01–0·7 mM) was added to the extracellular solution, the inward current was attenuated in a strongly concentration- and voltage-dependent manner. Figure 2*B* shows plots of the fraction of channels blocked $(1 - I_B/I_0)$, where the strong voltage dependence of the block appears as a steep region extending from −120 to −50 mV (0·01 mM) or −60 to −10 mV (2 mM). Using a Woodhull model (Woodhull, 1973), we quantified the voltage dependence of the block by transforming the blocked current into a linear form (eqn (2); Fig. 2*C*). The slope and the y-axis intercept of the fitted line to the linear region of these plots indicate the voltage dependence of the block, δ, and the voltage-independent affinity of Mg^{2+} for

the channel, $K_{0.5}$(0 mV), respectively. For wild-type channels, the voltage dependence as well as $K_{0.5}$(0 mV) was dependent on the concentration, being 0·58 and 0·8 mM in 0·01 mM Mg^{2+} and around 0·82 and 4·0 mM at 0·07 mM Mg^{2+} and higher concentrations (Table 1).

Since the extent of block depended strongly on concentration, different voltage ranges were used to quantify the voltage dependence of the block. For a simple Woodhull model, the parameters should be independent of membrane potential. The Woodhull block parameters are assumed to reflect a specific binding site in a channel, indicating its position in the transmembrane electric field (δ) and its intrinsic voltage-independent affinity. Nevertheless, given that they are concentration dependent, they must be viewed more cautiously at present.

A Woodhull model describes the block by 0·7 mM Mg^{2+} quite well over intermediate or physiological membrane potentials (~−70 to −10 mV; continuous line in Fig. 2*A*). However, at more negative potentials the block was weaker than that predicted, an effect seen in Fig. 2*C* where the block starting around −80 mV deviated upward from the line fitted over intermediate potentials. Hence, two regions of the block can be defined: over intermediate potentials (~−70 to −10 mV), the block followed a simple Woodhull model whereas at more negative potentials it deviated from this model. This deviation indicates that in addition to simple block other mechanism(s) are occurring which may be present over the entire voltage range but are dominant at negative potentials. One such mechanism is that the blocking particle passes through the channel.

Mg^{2+} permeation in wild-type NR1–NR2A channels

Mg^{2+} poorly permeates NMDA receptor channels (Mayer & Westbrook, 1987; Iino, Ozawa & Tsuzuki, 1990) indicating a large energy barrier to the inward transport of Mg^{2+}. Reversal potentials and relative chord conductances are indexes of this barrier. Figure 3*A* and *B* shows currents in wild-type channels in high K^+ or Mg^{2+}. In K^+, the currents were large and reversed near −5 mV. When Mg^{2+} replaced K^+, the currents were reduced at all potentials but a detectable inward current was observed negative to −52 mV (Fig. 3*A*, right panel), indicating that Mg^{2+} is less permeant than K^+. On average, replacing K^+ with Mg^{2+} produced a shift in the reversal potential of $-52 \pm 0{\cdot}4$ mV ($n = 7$). As an additional index of Mg^{2+} permeability in NMDA receptor channels, we compared the relative chord conductance in high Mg^{2+} (at −120 mV) to that in K^+ (at −40 mV); the percentage relative chord conductance, G_{Mg}/G_K, in wild-type was $0{\cdot}4 \pm 0{\cdot}1$ %. Thus, extracellular Mg^{2+} traverses the NMDA receptor channel but much less readily than K^+.

Given that Mg^{2+} carries a definable inward current (see also Stout, Li-Smerin, Johnson & Reynolds, 1996), Mg^{2+} must be viewed as a permeant blocker in wild-type channels where the extent of block by Mg^{2+} is a balance between its rate of entry and exit from the extracellular side (simple block) and passage through the channel (permeation) (French & Shoukimas, 1985). Consider the simplified blocking scheme:

$$Mg_o^{2+} + \text{site} \underset{k_{off}(E)}{\overset{k_{on}(E)}{\rightleftharpoons}} Mg^{2+}\text{–site} \xrightarrow{k'_{off}(E)} Mg_i^{2+} + \text{site}$$

Scheme 1

where the k values are the voltage-dependent rate constants, dependent on membrane potential (E), for Mg^{2+} entering (k_{on}) and exiting (k_{off}) a blocking site from the extracellular side or passing to the intracellular side (k'_{off}). (We have assumed that Mg_i^{2+} is negligible and does not contribute to the block under our recording conditions.) Channel block arises when Mg^{2+} occupies a blocking site. A simple voltage-dependent block process is defined in terms of $k_{on}(E)$ and $k_{off}(E)$ with the apparent affinity at any potential: $K_D(E) = k_{off}(E)/k_{on}(E)$, which is quantitatively described

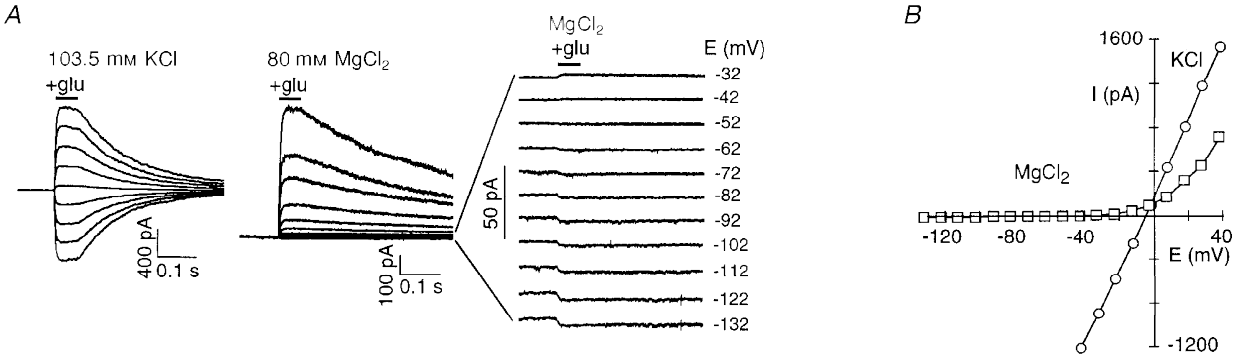

Figure 3. Mg^{2+} permeates wild-type NR1-NR2A channels

A, glutamate-activated currents at different membrane potentials in oocyte outside-out patches. Currents were generated by voltage steps, in 10 mV increments, and were recorded in patches bathed in high K^+ (from −42 to +38 mV) or high Mg^{2+} (−132 to +38 mV) with the pipette containing 123·5 mM K^+. Right panel, expanded traces recorded in Mg^{2+}. Glutamate (200 μM; glu) was added for the periods indicated by the horizontal bars. *B*, peak current–voltage relationship for records shown in *A*. The K^+ record is an average of the currents recorded before and after exposure to Mg^{2+}.

by a simple Woodhull model. However, permeation of Mg^{2+} adds another route by which Mg^{2+} can leave its blocking site, k'_{off}, and any measure of binding affinity will include this term: $K'_D(E) = (k_{off}(E) + k'_{off}(E))/k_{on}(E)$. Since we measured macroscopic currents in this study, we cannot define the individual rate constants. Nevertheless, three general points are noteworthy. First, inward Mg^{2+} permeation will quantitatively attenuate the extent of block by effectively reducing the dwell time of Mg^{2+} at its blocking site. Second, since all of the rate constants are voltage dependent, the effect of permeation on the block will be strongly dependent on membrane potential, becoming more prominent with negative potentials. Hence, at moderate potentials the situation may occur where $k_{off}(E) \gg k'_{off}(E)$, namely, that permeation does occur but does not significantly attenuate the block process at these potentials. Finally, we assume that Mg^{2+} permeation, as measured in Fig. 3, is an approximate index of k'_{off} but cannot quantitatively describe it. Since Mg^{2+} permeates wild-type channels poorly (Fig. 3), this process may not attenuate the block significantly, at least over physiological potentials, but additional information will be required to verify this point.

Extracellular Mg^{2+} block in channels containing glycine substituted for exposed residues at the narrow constriction

In considering how residues contribute to a blocking site, we initially examined the substitution of the small and non-polar glycine; this substitution removes any structural and energetic contribution a polar side chain would make to a blocking site and therefore would presumably attenuate the block. Figure 4*A–C* illustrates the block by extracellular Mg^{2+} in channels containing glycine substituted for any one of three asparagine residues positioned at (NR1(N0), NR2A(N + 1)) or external to (NR2A(N0)) the narrow constriction. For all three mutant channels, the current–voltage relationship in the absence of Mg^{2+} was linear, like

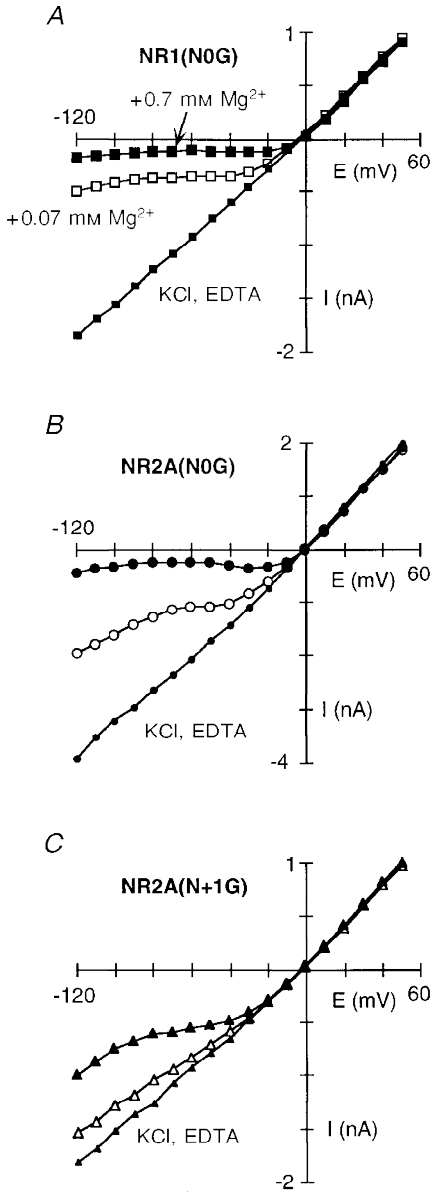

Figure 4. Mg^{2+} block in glycine-substituted channels
Extracellular Mg^{2+} block in NR1(N0G)–NR2A (*A*), NR1–NR2A(N0G) (*B*) and NR1–NR2A(N + 1G) (*C*) channels. Currents recorded and displayed as in Fig. 2*A*. Lines through the points in Mg^{2+} have no theoretical significance.

Table 2. Woodhull parameters for extracellular Mg^{2+} block of NMDA receptor channels containing mutant NR1-subunits

Subunit composition	$[Mg^{2+}]$ (mM)	δ	$K_{0.5}$(0 mV) (mM)
NR1(N0G)–NR2A	0·07	0·81 ± 0·03	1·5 ± 0·2
	0·7	0·82 ± 0·03	1·6 ± 0·1
NR1(N0S)–NR2A	0·07	0·80 ± 0·02	1·3 ± 0·1
	0·7	0·80 ± 0·01	1·6 ± 0·1
NR1(N0Q)–NR2A	0·07	0·88 ± 0·04	1·6 ± 0·2
	0·7	0·89 ± 0·02	2·8 ± 0·5
NR1(N0D)–NR2A	0·07	0·87 ± 0·04	0·29 ± 0·03
	0·7	—	—
NR1(N0R)–NR2A	0·07	—	—
	0·7	—*	—*

Six to eight experiments were performed for each set of parameters. See Table 1 for details. Except for the N0G (see Fig. 5*C* and *D*), fitted ranges were comparable to wild-type. * The current was blocked by less than 10 % at all potentials. Values are means ± S.E.M.

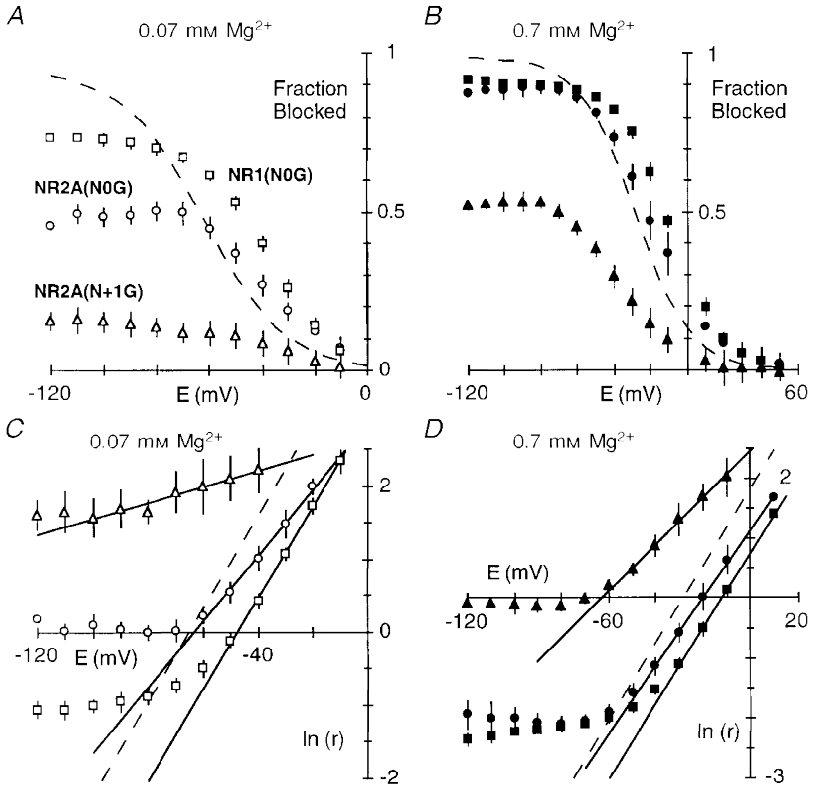

Figure 5. Voltage dependence of the block in glycine-substituted channels

A and *B*, comparison of the mean fraction blocked by 0·07 mM Mg^{2+} (*A*) or 0·7 mM Mg^{2+} (*B*) in NR1(N0G)–NR2A (squares), NR1–NR2A(N0G) (circles), and NR1–NR2A(N + 1G) (triangles) channels. Dashed lines are Boltzmann fits for wild-type (Fig. 2*B*). *C* and *D*, mean ln(*r*) in 0·07 mM Mg^{2+} (*C*) or 0·7 mM Mg^{2+} (*D*) for glycine-substituted channels (same symbols as *A* and *B*), compared with wild-type (dashed lines). Lines were fitted over the apparent linear region from *C*: NR1(N0G), −50 to −10 mV; NR2A(N0G), −60 to −20 mV; NR2A(N + 1G), −100 to −40 mV; and *D*: NR1(N0G), −30 to +10 mV; NR2A(N0G), −40 to +10 mV; NR2A(N + 1G), −50 to −10 mV.

Table 3. Woodhull parameters for extracellular Mg^{2+} block of NMDA receptor channels containing mutant NR2A-subunits

Subunit composition	$[Mg^{2+}]$ (mM)	δ	$K_{0.5}$(0 mV) (mM)
NR1–NR2A(N0G)	0·07	0·57 ± 0·03	1·2 ± 0·2
	0·7	0·72 ± 0·02	2·2 ± 0·2
NR1–NR2A(N0S)	0·07	0·62 ± 0·03	1·8 ± 0·3
	0·7	0·78 ± 0·02	3·5 ± 0·3
NR1–NR2A(N0Q)	0·07	0·41 ± 0·03	2·1 ± 0·1
	0·7	0·57 ± 0·02	4·5 ± 0·4
NR1–NR2A(N0D)	0·07	—	—
	0·7	—†	—†
NR1–NR2A(N0R)	0·07	—	—
	0·7	—*	—*
NR1–NR2A(N + 1G)	0·07	0·12 ± 0·03	1·0 ± 0·4
	0·7	0·50 ± 0·03	8·7 ± 1
NR1–NR2A(N + 1S)	0·07	0·32 ± 0·03	2·4 ± 0·2
	0·7	0·53 ± 0·04	9·1 ± 1·5
NR1–NR2A(N + 1Q)	0·07	0·42 ± 0·03	5·9 ± 1·5
	0·7	0·46 ± 0·02	7·8 ± 1·0
NR1–NR2A(N + 1D)	0·07	0·71 ± 0·02	1·5 ± 0·2
	0·7	0·80 ± 0·02	3·7 ± 0·4
NR1–NR2A(N +1R)	0·07	—	—
	0·7	—*	—*
NR1–NR2A(S + 2G)	0·07	0·80 ± 0·02	1·1 ± 0·2
	0·7	0·87 ± 0·02	1·8 ± 0·2

Four to seven experiments were performed for each set of parameters. See Table 1 for details. Fitted ranges were typically from −70 to −30 mV (0·07 mM) and −50 to −10 mV (0·7 mM). † Mg^{2+} block could not be quantified (see text for details). * The current was blocked by less than 10% at all potentials. Values are means ± S.E.M.

that in wild-type. Similarly, the addition of Mg^{2+} reduced the inwardly directed current but the extent of this attenuation differed from that in wild-type as well as between the mutant channels, being weakest in NR2A(N + 1G) (Fig. 4*C*).

A direct comparison of the fraction blocked by 0·07 or 0·7 mM Mg^{2+} in these mutant channels with that in wild-type (dashed lines) is shown in Fig. 5*A* and *B*. The extent of block relative to that in wild-type, whether it was enhanced or attenuated, and the magnitude of this difference, depended strongly on membrane potential. At negative potentials the block in all three mutant channels was weaker to varying degrees. On the other hand, at intermediate potentials (∼−50 to −10 mV), the pattern of block was different. In 0·07 mM Mg^{2+}, for example, the extent of block was enhanced in NR1(N0G) (open squares) as indicated by the rightward shift in the fraction blocked and remained steeply voltage dependent, in NR2A(N0G) (open circles) the block was also enhanced but to a lesser degree, and in NR2A(N + 1G) (open triangles) the block was nearly abolished. For all three mutant channels, the block over intermediate potentials was voltage dependent as quantified in Fig. 5*C* (0·07 mM) and Fig. 5*D* (0·7 mM). In NR1(N0G), the linear region was shifted to more positive potentials compared with wild-type (dashed line), but the voltage dependence of the block, around 0·80 in 0·07 or 0·7 mM Mg^{2+}, was unchanged (Table 2). In contrast, for NR2A(N0G) and NR2A(N + 1G), the voltage dependence was attenuated. However, the extent of the attenuation depended on the Mg^{2+} concentration, being more strongly reduced in 0·07 mM Mg^{2+}. In NR2A(N + 1G), for example, the voltage dependence was reduced to 0·50 in 0·7 mM Mg^{2+} but to nearly 0·12 in 0·07 mM Mg^{2+}.

The voltage dependence of the block by 0·07 and 0·7 mM Mg^{2+} for the NR1(N0G), NR2A(N0G) and NR2A(N + 1G) channels as well as NR2A(S + 2G) compared with that in wild-type is summarized in Fig. 6. In NR1(N0G) and NR2A(S + 2G), the voltage dependence of the block was similar at both concentrations and comparable to that in wild-type. In contrast, for the two adjacent NR2A-subunit asparagines the voltage dependence was attenuated, with this attenuation being more prominent at 0·07 mM Mg^{2+} and in NR2A(N + 1G) channels. Thus, removing the side chain at either NR2A(N0) or NR2A(N + 1) disrupts the block over physiological potentials but much more strongly at N + 1 suggesting that the two asparagines contribute but not equally to a blocking site.

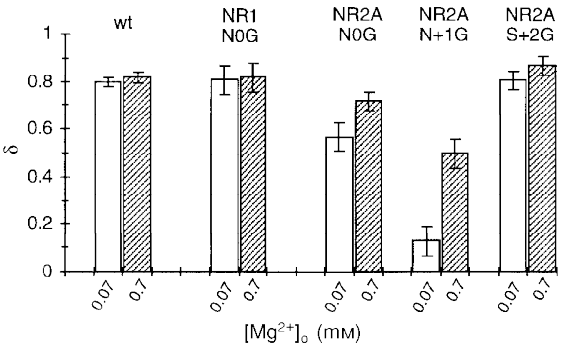

Figure 6. Attenuation of the voltage dependence of block in channels containing glycine substituted at NR2A(N0) or NR2A(N + 1) is concentration dependent
Mean voltage dependence of the block, δ, in glycine-substituted channels. Values are shown as means ± 2 S.E.M. wt, wild-type.

Substitution of glutamine for the adjacent NR2A-subunit asparagines but not the NR1-subunit N-site attenuates the block by Mg^{2+}

Glycine is an extreme substitution, completely removing the side chain at the substituted position. Glutamine (Q) differs from the native asparagine only in an added methylene group, and substitution of it would primarily alter the geometric relationship of side chains leaving the chemically important amide group intact. A comparison of the block in channels containing glutamine substituted for any one of the three asparagines is shown in Fig. 7*A–C*. In NR1(N0Q) (Fig. 7*A*), the block by Mg^{2+} was comparable to that in wild-type. In contrast, the block in channels containing glutamine substituted in the NR2A-subunit at N0 (Fig. 7*B*) or N + 1 (Fig. 7*C*) was strongly attenuated. Figure 8*A* shows the fraction blocked by 0·7 mM Mg^{2+} in these

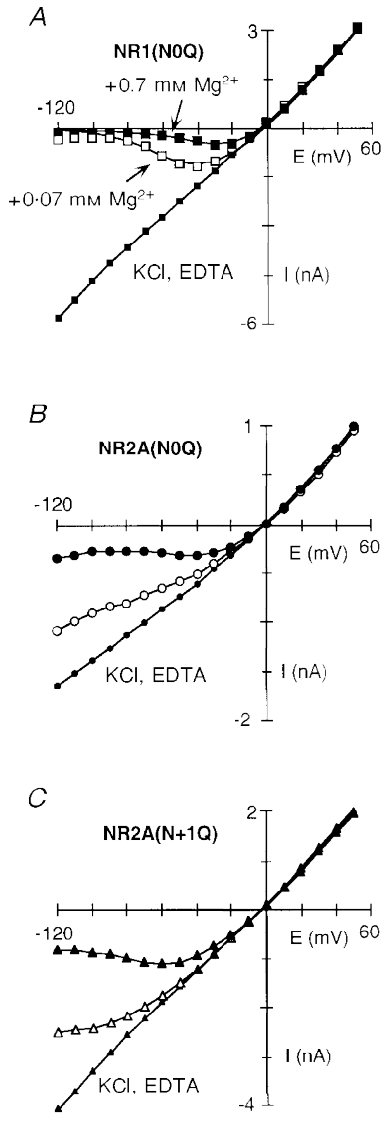

Figure 7. Mg^{2+} block in glutamine-substituted channels
Extracellular Mg^{2+} block in NR1(N0Q)–NR2A (*A*), NR1–NR2A(N0Q) (*B*) and NR1-NR2A(N + 1Q) (*C*) channels. Currents recorded and displayed as in Fig. 2*A*. The continuous lines through the points in Mg^{2+} for NR1(N0Q) are from eqn (1) with the parameters δ and $K_{0.5}$(0 mV) derived from eqn (2). For NR2A(N0Q) and NR2A(N + 1Q), the lines through the Mg^{2+} points have no theoretical significance.

glutamine-substituted channels. In the case of NR1(N0Q) (squares), the extent of block at any one potential was enhanced relative to that in wild-type (dashed line) but the voltage dependence of the block, around 0·88, was comparable (Fig. 8*B*; Table 2). On the other hand, in NR2A(N0Q) (circles) and NR2A(N + 1Q) (triangles), the block was reduced over the entire voltage range. At intermediate potentials, this attenuation was stronger in NR2A(N + 1Q) than in NR2A(N0Q). At very negative potentials this pattern was reversed. The voltage dependence of the block in these NR2A mutant channels was also reduced (Fig. 8*B*). Like the glycine substitutions, this attenuation was concentration dependent but the difference was greater in NR2A(N0Q) than in NR2A(N + 1Q). Indeed, in both mutant channels, the voltage dependence of the block was reduced to around 0·41 at 0·07 mM, whereas at 0·7 mM it was reduced to about the same extent for NR2A(N + 1Q) but only to 0·57 in NR2A(N0Q) (Table 3).

In summary, the glutamine substitution further distinguishes the contribution of the asparagines to extracellular Mg^{2+} block. In the case of NR1(N0Q), the extent of block was enhanced but its voltage dependence was essentially unchanged. Indeed, as summarized in Table 2, all NR1(N0) substitutions, except for the positively charged arginine (R) which essentially abolishes the block, produced comparable effects on the block enhancing it over intermediate potentials but leaving the voltage dependence intact. On the other hand, substitution of glutamine at NR2A(N0) or NR2A(N + 1) strongly attenuated the extent as well as the voltage dependence of the block. This result is consistent with the amino acid residues at these positions contributing to the mechanism for Mg^{2+} block and also suggest that the geometric relationship of exposed side chains in the lumen is important.

In the NR2A-subunit, the N + 1 site asparagine is a more important determinant of Mg^{2+} block than the N-site asparagine

Table 3 compares the Woodhull parameters for the block of channels containing identical substitutions of the adjacent NR2A-subunit asparagines including glycine and glutamine as well as the polar serine (S) and the negatively charged aspartate (D). Substitution of serine at either NR2A(N0) or NR2A(N + 1) produced similar effects on the block as the glycine and glutamine substitutions; the voltage dependence was attenuated in a concentration-dependent manner with a much stronger attenuation in NR2A(N + 1S). Indeed, substitution of glycine, serine and glutamine at the N + 1 site consistently produced a stronger disruption of the block than the equivalent substitution at the N-site indicating that the N + 1 site represents a more important structural determinant of the block than the N-site. The block in channels containing aspartate at NR2A(N + 1) was also concentration dependent; surprisingly, however, the extent of block was not strongly enhanced, an issue we return to in the Discussion.

Substitution of aspartate at NR2A(N0) produced channels which yielded small currents. Also, in the absence of Mg^{2+} these channels showed a strong inward rectification and a time-dependent increase in the current amplitude with voltage steps to negative potentials; a more complex current pattern occurred in the presence of Mg^{2+}

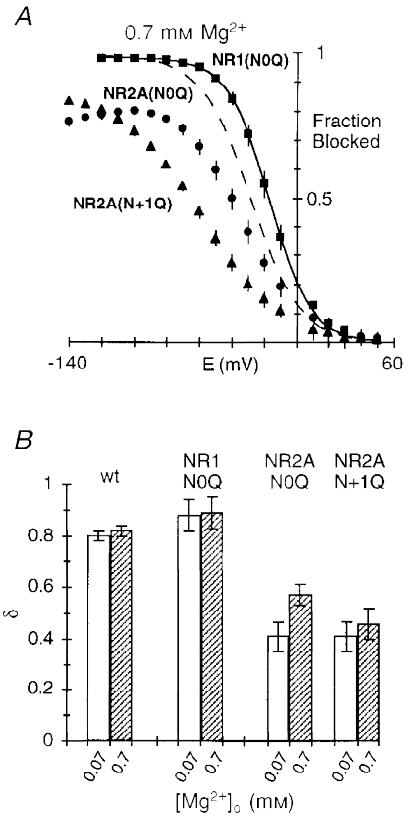

Figure 8. Voltage dependence of the block in glutamine-substituted channels

A, comparison of the mean fraction blocked by 0·7 mM Mg^{2+} in NR1(N0Q)–NR2A (■), NR1–NR2A(N0Q) (●), and NR1–NR2A(N + 1Q) (▲). Dashed line is wild-type (Fig. 2*B*). *B*, mean voltage dependence of the block, δ, in glutamine-substituted channels. Values are shown as means ± 2 S.E.M.

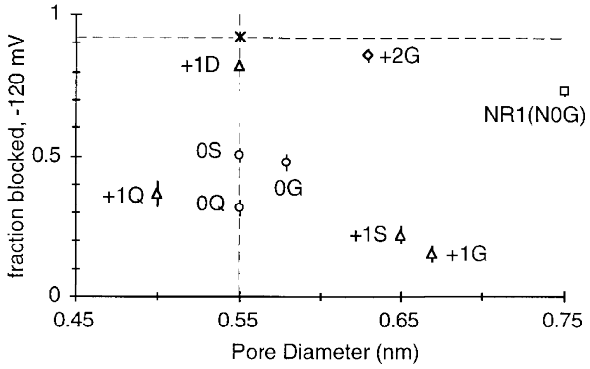

Figure 9. Mg^{2+} blocks NMDA receptor channels independent of pore size

Fraction blocked by 0·07 mM Mg^{2+} at −120 mV plotted against pore diameter for wild-type (asterisk) and mutant NR2A channels (except for NR1(N0G)). The dashed lines are shown to indicate the values that would be observed if only one property, pore size (horizontal line) or Mg^{2+} block (vertical line), was changed.

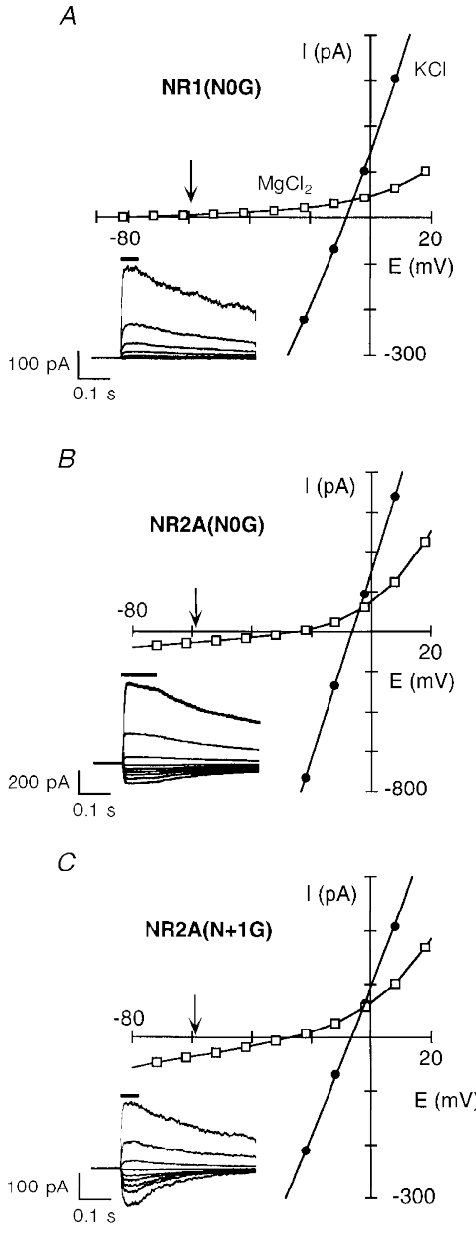

Figure 10. Inward Mg^{2+} permeability in glycine-substituted channels

Glutamate-activated currents recorded as in Fig. 3*A* and *B* except that outside-out patches were isolated from oocytes expressing NR1(N0G)–NR2A (*A*), NR1–NR2A(N0G) (*B*), or NR1–NR2A(N + 1G) (*C*) channels. The arrow in each plot indicates the expected reversal potential in Mg^{2+} given the observed reversal potential in the K^+ solution and the average change in reversal potential for wild-type channels, ∼−52 mV. For NR1(N0G)–NR2A channels, currents in Mg^{2+} reversed around −77 mV. Insets, glutamate-activated currents in the presence of 80 mM $MgCl_2$ shown in 20 mV increments (from −82 to +18 mV).

Table 4. ΔE_r and relative chord conductance for Mg^{2+} measured in wild-type and mutant NR1–NR2A NMDA receptor channels

Subunit composition	ΔE_r (mV)	G_{Mg}/G_K (%)	n
NR1–NR2A	−51·4 ± 0·4	0·4 ± 0·1	7
NR1(N0G)–NR2A	−70·9 ± 1	0·6 ± 0·1	6
NR1(N0S)–NR2A	< −127	—	5
NR1(N0D)–NR2A	−61·6 ± 1·5	0·7 ± 0·2	5
NR1(N0Q)–NR2A	−50·1 ± 1·4	0·6 ± 0·2	3
NR1–NR2A(N0G)	−18·0 ± 0·3	1·6 ± 0·2	5
NR1–NR2A(N0S)	−30·0 ± 0·7	2·3 ± 0·2	5
NR1–NR2A(N0Q)	−23·5 ± 1	4·0 ± 0·5	7
NR1–NR2A(N + 1G)	−21·9 ± 0·8	8·9 ± 1	8
NR1–NR2A(N + 1S)	−13·9 ± 0·4	14·6 ± 3	8
NR1–NR2A(N + 1D)	−43·3 ± 0·5	2·1 ± 0·1	4
NR1–NR2A(N + 1Q)	−58·1 ± 0·4	3·0 ± 0·3	5
NR1–NR2A(S + 2G)	−43·3 ± 0·6	0·6 ± 0·1	7

Reference solution (mM): 103·5 KCl, 10 Hepes, 0·18 $CaCl_2$ (oocyte macropatches) or 103·5 KCl, 10 Hepes (HEK 293 cells). Test solution (mM): 78 $MgCl_2$, 2 $Mg(OH)_2$, 10 Hepes. Results from oocyte outside-out patches and HEK 293 whole-cell recordings were indistinguishable and were combined. Current amplitudes used to calculate relative chord conductances were measured at −120 mV (high Mg^{2+}) or −40 mV (high K^+). Values are means ± S.E.M.

making quantification of the block difficult. We therefore did not explore Mg^{2+} block in this mutant channel.

The narrow constriction is not a steric barrier for Mg^{2+}

The NR2A(N + 1) site, in contrast to the NR2A(N0) site, contributes to the size of the narrow constriction (Wollmuth *et al.* 1996). Since substitutions at NR2A(N + 1) alter pore size, the stronger effects of substitutions at this position on the block could reflect the possibility that the underlying mechanism of the block by Mg^{2+} is steric occlusion. If Mg^{2+} block is determined by steric occlusion of the channel lumen rather than by energetic factors, the extent of block especially at very negative potentials should be inversely related to pore diameter. However, as shown in Fig. 9, any such relationship was limited. Clearly, channels containing the NR2A(N + 1G) or NR2A(N + 1S) substitutions (open triangles) had an increased pore diameter as well as an attenuated block. However, the block was also attenuated in channels where pore diameter was reduced, NR2A(N + 1Q) (open triangles), or unchanged, NR2A(N0Q) and NR2A(N0S) (open circles). Further, pore diameter was greatly increased in NR2A(S + 2G) (open diamonds) and in NR1(N0G) (open squares) yet block was weakly affected. Hence, pore diameter *per se* does not determine how strongly Mg^{2+} blocks mutant NMDA receptor channels suggesting that the energetics of the side chains positioned at the narrow constriction contribute to the block. This energetic contribution could arise by a direct interaction of Mg^{2+} with the adjacent asparagines (binding) and/or the adjacent asparagines could act as an energy barrier for Mg^{2+} influx.

Adjacent asparagines in the NR2A-subunit form an energy barrier for Mg^{2+} influx

In channels containing glycine substituted at NR1(N0), NR2A(N0) or NR2A(N + 1), the block by Mg^{2+} was weaker at negative potentials than in wild-type (Fig. 4). Such behaviour could reflect the possibility that Mg^{2+} acts as a stronger permeant blocker in these mutant channels than in wild-type. To test this possibility, we measured the apparent changes in reversal potential and relative chord conductance in high Mg^{2+} for these glycine-substituted channels. Quantitatively, any relationship between these indexes of Mg^{2+} permeability and block cannot be made since the substitutions may affect K^+ as well as Mg^{2+} flux, and these indexes measured in 80 mM Mg^{2+} may overestimate the magnitude of the Mg^{2+} influx at low Mg^{2+} concentrations (Stout *et al.* 1996). Nevertheless, we anticipate that if an increased influx contributes to the attenuated block, a qualitative relationship between Mg^{2+} influx and block should exist.

Figure 10 shows current–voltage relationships in high K^+ or Mg^{2+} for the glycine-substituted channels. In NR1(N0G) (Fig. 10*A*), the reversal potential in high Mg^{2+} was shifted to more negative potentials than in wild-type (arrow), suggesting that Mg^{2+} crosses this mutant channel less readily. Hence, the attenuated block at very negative potentials in NR1(N0G) apparently does not reflect an increased Mg^{2+} influx. Evidence consistent with this idea is that the fraction blocked, though attenuated relative to wild-type at negative potentials, became stronger with more

negative potentials (see Fig. 5*A* and *B*). We have not explored further the basis of this attenuated block in NR1(N0G) but note that the breakthrough of current in Mg^{2+} at negative potentials (see Fig. 4*A*) cannot be explicitly ascribed to permeation.

An alternative explanation for the lack of effect on Mg^{2+} influx is that the NR1(N0G) substitution enhanced K^+ flux, shifting the reversal of the net current in high Mg^{2+} in a negative direction. If this is true, a similar reduced Mg^{2+} efflux should be seen from the internal face of the channel (the reversal should be shifted positive relative to wild-type). However, the opposite occurred (see Fig. 14*A* of Wollmuth *et al.* 1998), consistent with the idea that Mg^{2+} influx is not strongly enhanced in NR1(N0G).

In contrast to NR1(N0G), both NR2A(N0G) (Fig. 10*B*) and NR2A(N + 1G) (Fig. 10*C*) have a reversal potential in Mg^{2+} relative to wild-type which was shifted towards zero suggesting that Mg^{2+} permeates more readily. G_{Mg}/G_K was also increased in both mutant channels compared with wild-type (Table 4). The rightward shift in the reversal potential and the increase in G_{Mg}/G_K are consistent with Mg^{2+} acting as a stronger permeant blocker in these mutant channels than in wild-type. However, the shift in the reversal potential was more positive in NR2A(N0G) (~−18 mV) than in NR2A(N + 1G) (~−22 mV), yet the block was more strongly attenuated in NR2A(N + 1G) (see Fig. 5*A* and *B*). Nevertheless, the increase in G_{Mg}/G_K, nearly twentyfold in NR2A(N + 1G) but only fourfold in NR2A(N0G), inversely paralleled the reduction in the extent of block. Thus, G_{Mg}/G_K appears to reflect, at least qualitatively, how permeation influences the extent of block.

Table 4 summarizes ΔE_r and G_{Mg}/G_K for all substitutions tested. In NR1(N0)-substituted channels, ΔE_r in high Mg^{2+}, like that in N0G, tended to be reduced with the serine substitution producing channels where no inward current in high Mg^{2+} could be detected up to −127 mV. In contrast, substitutions of either adjacent NR2A-subunit asparagine but not the NR2A(S + 2) serine enhanced the apparent driving force for Mg^{2+}, relative chord conductance or both. Thus, the adjacent NR2A-subunit asparagines, but not the NR1-subunit N-site asparagine or the NR2A(S + 2) serine, contribute to a barrier for inward Mg^{2+} permeability. In this regard, therefore, a function of the adjacent asparagines is to maintain a low k'_{off} (Scheme 1).

Substitutions of the adjacent asparagines in the NR2A-subunit produced the strongest effect on the increase in inward Mg^{2+} permeability and attenuation of the block. Since Mg^{2+} influx attenuates the extent of block, the function of the adjacent NR2A-subunit asparagines in the block mechanism could be to act solely as a barrier for Mg^{2+} influx (i.e. they contribute to the maintainance of a low k'_{off} in Scheme 1 without contributing to k_{off} or k_{on}). However, in mutant NR2A channels, the relationship between the extent of block and ΔE_r which can be interpreted as an index of the barrier for Mg^{2+} influx, was poor (data not shown). In addition, the extent of block at −120 mV showed a good correlation with G_{Mg}/G_K, indicating that this index of Mg^{2+} influx reflects elements of the block process. However, over intermediate potentials (~−70 to −10 mV), no correlation existed suggesting that processes in addition to changes in Mg^{2+} influx were being altered in these mutant channels. Quantitatively, we cannot state the relative contribution of these different processes at different potentials, but additional evidence is presented below which suggests that, over intermediate potentials (~−40 to −10 mV), the contribution of inward Mg^{2+} permeability to the block in mutant NR2A channels is small.

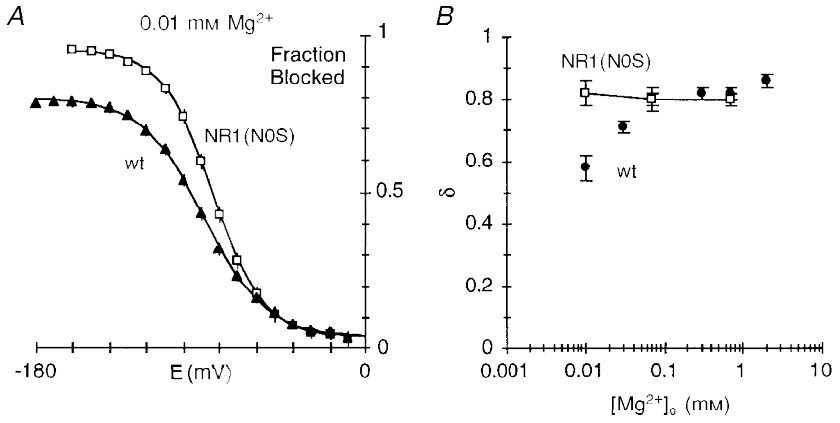

Figure 11. Mg^{2+} influx contributes to the attenuation of δ at low concentrations in wild-type

A, comparison of the mean fraction blocked by 0·01 mM Mg^{2+} in NR1(N0S)–NR2A (□) and wild-type (▲). The continuous lines are the Boltzmann equation (eqn (3)) fitted over the entire voltage range. Parameters: wild-type: B_{max}, 76·6; $E_{0.5}$, −88·7 mV; $z\delta$, 1·48; and NR1(N0S): B_{max}, 91·9; $E_{0.5}$, −83·8 mV; $z\delta$, 1·83. In ln(r) plots for NR1(N0S), the line was fitted over −100 to −60 mV as in wild-type. *B*, mean voltage dependence of the block, δ, at different Mg^{2+} concentrations in NR1(N0S)–NR2A (□) or wild-type (●) channels.

Mg^{2+} influx contributes to the attenuation of δ in wild-type at low Mg^{2+} concentrations

In wild-type, the voltage dependence of the block by 0·01 mM Mg^{2+}, which could be quantified only over negative potentials (Fig. 2*C*), was attenuated relative to that at higher concentrations. Permeation of a blocking ion reduces the apparent voltage dependence of the block (French & Shoukimas, 1985). Substitution of serine at NR1(N0) produced channels where no inward current in high extracellular Mg^{2+} could be detected (Table 4). To test the idea that Mg^{2+} influx attenuates the voltage dependence of the block by 0·01 mM Mg^{2+}, we quantified the block in NR1(N0S)–NR2A channels at this concentration (Fig. 11). The fraction blocked by 0·01 mM Mg^{2+} in NR1(N0S) is compared with that in wild-type in Fig. 11*A*. Up to −60 mV the block was indistinguishable in the two channel types, but starting at −70 mV the extent of block diverged, becoming stronger in NR1(N0S). In addition, the block was more steeply voltage dependent in NR1(N0S) yielding a δ of $0{\cdot}82 \pm 0{\cdot}02$ ($n = 5$). A comparison of δ as a function of concentration in NR1(N0S) and wild-type channels is shown in Fig. 11*B*. In contrast to wild-type, δ showed no concentration dependence in NR1(N0S), being independent of membrane potential. This result is consistent with the idea that in wild-type Mg^{2+} influx attenuates the voltage dependence of the block at negative potentials.

The adjacent asparagines in the NR2A-subunit contribute to the mechanism controlling the strong voltage dependence of the block

Substitutions of the adjacent asparagines in the NR2A-subunit strongly reduced the voltage dependence of the block as well as increased the apparent Mg^{2+} influx. To test whether an increased Mg^{2+} influx is the only mechanism underlying the reduced voltage dependence of the block in mutant NR2A channels, we examined the block in these channels in two additional ways. First, we measured the block by a wider concentration range of Mg^{2+} in NR2A(N0Q) and NR2A(N + 1G). These substitutions were selected for this analysis since at the respective positions they showed the most strongly reduced block. We anticipated that if Mg^{2+} influx is the sole mechanism attenuating the voltage dependence then there would be a continuous increase in δ at higher concentrations. However, as shown in Fig. 12*A*, this was not the case. In particular, for NR2A(N0Q) (open circles) the voltage dependence of the block reached a plateau starting at 0·3 mM Mg^{2+} ($\delta = 0{\cdot}54 \pm 0{\cdot}04$, $n = 5$) without becoming any stronger in 0·7 Mg^{2+} ($\delta \approx 0{\cdot}57$) or 2 mM Mg^{2+} ($\delta = 0{\cdot}50 \pm 0{\cdot}01$, $n = 5$). Similarly, for NR2A(N + 1G) (triangles), the voltage dependence again reached a plateau at higher Mg^{2+} concentrations though this effect occurred at 0·7 mM ($\delta \approx 0{\cdot}50$) and 2 mM Mg^{2+} ($\delta = 0{\cdot}53 \pm 0{\cdot}03$, $n = 7$).

The second approach we used was to quantify the derivative of ln(r) plots in 0·7 mM Mg^{2+} (Fig. 12*B*). This analysis is identical to that shown in Fig. 2*C* but δ was now based on the slope at a single voltage rather than a range of voltages. In wild-type (filled circles), the derivative of ln(r) was around 0·8 between −60 and −10 mV and was strongly reduced at more negative potentials. A constant δ could reflect that between −60 and −10 mV either Mg^{2+} influx influences the block to an equivalent extent or that it contributes little to the block. Other results (Fig. 11) are consistent with the latter alternative. In all mutant NR2A channels, a constant δ was found but this occurred over a more limited voltage range than expected for channels where Mg^{2+} is more permeant. In NR2A(N0Q), for example, δ was around 0·57 between −40 and −10 mV but at potentials negative to −40 mV it was strongly reduced (Fig. 12*B*, open circles). Hence we assume that between

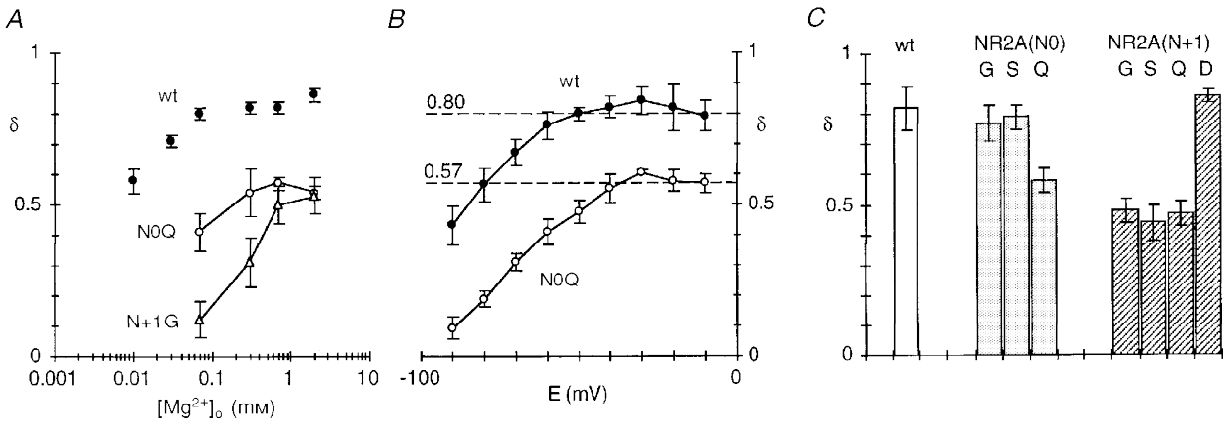

Figure 12. Voltage dependence of block in mutant NR2A channels

A, mean voltage dependence of the block, δ, at different Mg^{2+} concentrations in NR1–NR2A(N0Q) (○), NR1–NR2A(N + 1G) (△) or wild-type (●) channels. *B*, mean voltage dependence of the block, δ, measured at single potentials (i.e. the derivative of ln(r) plots) in NR1–NR2A(N0Q) (○) or wild-type (●) channels. *C*, mean voltage dependence of the block, δ, at −20 mV in 0·7 mM Mg^{2+} for channels containing NR2A(N0) or NR2A(N + 1) substitutions.

~−40 and −10 mV the primary escape route for Mg^{2+} from its blocking site is to the extracellular side (simple block, i.e. $k_{off} \gg k'_{off}$ in Scheme 1), and that measured values of δ over this voltage range are an index of the block process ($K_D(E)$ rather than $K'_D(E)$). A comparison of δ based on the derivative at −20 mV for substitutions at NR2A(N0) and NR2A(N + 1) to that in wild-type is shown in Fig. 12*C*. The values are comparable to those shown in Table 2 and indicate that the N + 1 site asparagine is a more important determinant of the mechanism underlying the voltage dependence of the block than the N-site asparagine.

In summary, the adjacent NR2A-subunit asparagines contribute to a barrier for Mg^{2+} influx. They also contribute to some other process in the block mechanism, possibly binding and/or the mechanism controlling the strong voltage dependence of the block. In mutant NR2A channels, this other process disrupts the block over the entire voltage range whereas at negative potentials, the block is further reduced by an increased permeation.

DISCUSSION

Our results demonstrate that the narrow constriction of NMDA receptor channels forms a structural determinant of the block by extracellular Mg^{2+}. However, residues forming the narrow constriction contribute differentially to the block. The NR1-subunit N-site asparagine and the NR2A-subunit S + 2 serine, while determining the dimensions of the narrow constriction (Wollmuth *et al.* 1996), appear to contribute little. In contrast, the N-site and the N + 1 site asparagines in the NR2A-subunit represent critical determinants of a blocking site. Previous work has shown that the N-site in the NR2-subunit is one determinant of the block (Burnashev *et al.* 1992; Mori, Masaki, Yamakura & Mishina, 1992; Sakurada, Masu & Nakanishi, 1993). We found that the two adjacent asparagines in the NR2A-subunit do not contribute equally to the blocking site, with the N + 1 site asparagine representing the more important determinant.

Mg^{2+} block and permeation in wild-type channels

Physiological concentrations of Mg^{2+} are around 1 mM. In 0·7 mM Mg^{2+}, the Woodhull model described the block in wild-type quite well over physiological potentials (~−70 to −10 mV; Fig. 2*A* and *C*). Starting around −80 mV, however, the block was weaker than that expected. At very low concentrations (0·01 and 0·03 mM) where the block could be quantified only at potentials negative to −40 mV, the voltage dependence of the block was attenuated relative to that at higher concentrations (Table 1). One possible explanation for the deviation from the Woodhull model and the reduced voltage dependence at low concentrations is that at negative potentials Mg^{2+} passes through the channel more readily, reducing the effective dwell time of Mg^{2+} at its blocking site. Consistent with this idea, we found an inward current in high extracellular Mg^{2+} in wild-type (Fig. 3), and native NMDA receptor channels have been shown to transport Mg^{2+} inwardly (Stout *et al.* 1996). Further, in NR1(N0S)–NR2A channels, where no inward current in the presence of high Mg^{2+} could be detected, the voltage dependence of the block by 0·01 mM Mg^{2+} was independent of Mg^{2+} concentration (Fig. 11*B*). Comparison of the block by 0·01 mM Mg^{2+} in wild-type and NR1(N0S)–NR2A channels (Fig. 11*A*) suggests that up to −60 mV permeation does not significantly attenuate the block. Hence, two regions of the block in wild-type can be defined. Over the physiological range (~−60 to −10 mV), the predominant escape route for Mg^{2+} from its blocking site is to the extracellular side (simple block). Consistent with this idea is that the Woodhull block parameters showed little concentration dependence between 0·07 and 0·7 mM Mg^{2+} where the block could be quantified over this potential range. At potentials negative to −60 mV, Mg^{2+} can now leave its blocking site and translocate to the cytoplasmic side of the channel. The attenuated current at these negative potentials in Mg^{2+} is therefore a combination of simple block by Mg^{2+} and weak permeation which reduces the block.

The estimated voltage-independent affinity for the channel, $K_{0.5}$(0 mV), is also influenced by permeation. In 0·01 mM Mg^{2+}, for example, permeation reduces the extent of block at negative but not intermediate potentials. This flattens out the fitted curve leading to a reduced voltage dependence and a lower y-axis intercept (i.e. a higher apparent affinity). We therefore compared $K_{0.5}$(0 mV) in mutant channels only in 0·7 mM Mg^{2+} where the block could be quantified between −60 and −10 mV.

Asparagines forming the narrow constriction contribute differently to Mg^{2+} block

The homologous N-site asparagines in the two subunits are positioned at the tip of the loops formed by the M2 segments. The narrowest part of the channel is, however, determined primarily by the non-homologous NR1-subunit N-site and NR2A-subunit N + 1 site asparagines (Kuner *et al.* 1996; Wollmuth *et al.* 1996). The strong effects of substitutions of the adjacent asparagines in the NR2A-subunit on the alteration of both the extent and voltage dependence of the block suggest that they form a structure critical for the block. In addition, based on identical substitutions, the N + 1 site asparagine is a more critical determinant of the block than the N-site asparagine. On the other hand, substitutions at the NR1-subunit N-site asparagine or the NR2A-subunit S + 2 serine had no effect on the voltage dependence of the block, altering only the extent of block at any one potential.

Mechanism of interaction of Mg^{2+} with the adjacent asparagines in the NR2A-subunit

One issue that remains to be resolved for the development of a molecular description of the block mechanism is the method by which Mg^{2+} interacts with the two adjacent asparagines in the NR2A-subunit. Three extreme possibilities will be considered. (a) The adjacent NR2A-subunit asparagines could represent simply an energy barrier for Mg^{2+} inflow. Here, Mg^{2+} would bind to residues at a distance from the narrow constriction with the adjacent asparagines acting as

a translocation barrier for Mg^{2+} inflow. Alternatively (b), the polar asparagine side chains could act as water substitutes specifically binding to Mg^{2+}. Finally (c), the narrow constriction could mediate the unknown mechanism controlling the strong voltage dependence of the block.

The adjacent asparagines represent an energy barrier for Mg^{2+} influx. At least part of the contribution of the adjacent asparagines to the block mechanism is to act as an energy barrier for Mg^{2+} influx since substitutions of them increased the apparent inward Mg^{2+} permeability (Table 4). Thus, a function of the adjacent asparagines is to maintain a small k'_{off} in Scheme 1, with the result that extracellular Mg^{2+} acts as a simple blocker over physiological potentials. This contribution is critical for the function of NMDA receptor channels. If k'_{off} was high in wild-type channels, at the resting membrane potential, typically −60 to −70 mV, NMDA receptor channels would carry a significant amount of inward current during a single EPSP (e.g. Figs 4*C* and 7*B*). This would prevent the NMDA receptor from acting as a detector of post-synaptic depolarization.

How do the adjacent asparagines prevent Mg^{2+} from crossing the channel? One possibility is that they form a steric barrier for Mg^{2+}. Since Mg^{2+} is a small ion (diameter, ∼0·13 nm; Frausto da Silva & Williams, 1991), giving it a large charge to surface area ratio, the removal of its inner hydration shell would require considerable free energy and its effective size would be considerably larger, at least 0·7 nm. Since NMDA receptor channels have a pore size of about 0·55 nm (Villarroel *et al.* 1995; Zarei & Dani, 1995; Wollmuth *et al.* 1996), hydrated Mg^{2+} could block NMDA receptor channels at the narrow constriction by steric occlusion. However, the relationship between how substitutions change pore size and block by Mg^{2+} is poor (Fig. 9). In addition, the strong increase in the apparent Mg^{2+} permeability in channels where no change in pore size occurred (e.g. NR2A(N0Q), NR2A(N0S)) suggests that Mg^{2+} crosses the narrow constriction in a partially dehydrated state. Hence, the energetics of the interaction between the narrow constriction and Mg^{2+} rather than its dimensions determines its function in Mg^{2+} block.

The adjacent asparagines form an energy barrier for Mg^{2+} influx. Various lines of evidence suggest, however, that they participate in the block mechanism in additional ways. First, no correlation between the extent of block at intermediate potentials and Mg^{2+} influx was found. Second, many of the substitutions, especially those of the N + 1 site, strongly altered the apparent voltage-independent affinity (Table 3). Finally, analysis of the block over intermediate potentials suggested that processes in addition to changes in permeation were occurring (Fig. 12).

We cannot quantitatively state the relative contribution of permeation without single channel analysis which will be required to define the effect of substitutions on the microscopic rate constants. However, analysis of how substitutions affect the block must explicitly consider permeation, which adds another route by which Mg^{2+} can leave its blocking site, k'_{off} (see Scheme 1), an effect that is especially strong at negative potentials (< −60 mV). Potentials at which to study the block at the single channel level must be selected carefully since a decrease in the dwell time does not necessarily reflect a change in binding but rather a change in inward permeability.

The adjacent asparagines represent a binding site for extracellular Mg^{2+}. Given the polar nature of the asparagine side chain, an ion-dipole co-ordination would underlie this interaction as illustrated in Fig. 13. Such a conclusion for the N + 1 site seems reasonable since substitution of glycine, serine or glutamine at this position attenuated $K_{0·5}$(0 mV) in 0·7 mM Mg^{2+} (Table 3). Nevertheless, the addition of a negative charge to a co-ordinating ligand typically enhances the strength of a co-ordination complex (Frausto da Silva & Williams, 1991; Falke, Drake, Hazard & Peersen, 1994). Substitution of the negatively charged aspartate at the N + 1 site, however, did not strongly enhance the block (Table 3). One possible explanation for this is that a negatively charged side chain at N + 1 forms a salt bridge with other side chains in the vicinity removing it from any interaction with Mg^{2+}. Alternatively, binding of Mg^{2+} to residues at the narrow constriction could depend both on the ligand type as well as on their spatial configuration. Consistent with this idea is that substitution of glutamine, which alters the geometry but not the ligand type of the native asparagine side chain, at NR2A(N + 1) strongly disrupts the block. Hence, the carboxylate side chain at N + 1 could alter this 'optimal' structural relationship. The weakly enhanced block in NR2A(N + 1D) channels therefore would be the net effect of increased binding due to the negative charge and decreased binding due to changes in the spatial relationship between ligands.

Binding of Mg^{2+} to the less critical NR2A-subunit N-site is also not clear cut. Substitution of glycine or serine at this site actually weakly enhanced the extent of block over intermediate potentials (Table 3). Nevertheless, others have concluded that the N-site in the NR2A-subunit does contribute to Mg^{2+} binding (Sharma & Stevens, 1996), based in part on a parallel reduction in the block over the entire voltage range in NR2A(N0Q) channels. In addition, these authors suggested that other structural elements must also participate in binding Mg^{2+}; this additional element is most probably the N + 1 site asparagine.

The parallel reduction in the block in NR2A(N0Q) seen by Sharma & Stevens (1996) differs from our observations in that for our comparable parameter, the fraction blocked, the deviation from wild-type depended strongly on membrane potential (Fig. 8*A*, circles). The basis for this divergent result is unknown but might be due to the different recording conditions. We recorded the block in high extracellular K^+ and in the complete absence of extracellular Ca^{2+} (EGTA externally) whereas Sharma & Stevens (1996) analysed the block in high extracellular Na^+ and in 0·1 mM Ca^{2+}.

The adjacent asparagines mediate the mechanism controlling the strong voltage dependence. A key feature of the block by extracellular Mg^{2+} is its strong voltage dependence, manifested at the single channel level as increasingly longer dwell times with more negative

potentials. The Woodhull model identifies the relative location of a blocking site (δ) in the transmembrane electric field based on the voltage dependence of the block. The voltage dependence of the block by Mg^{2+} in physiological solutions (e.g. Ascher & Nowak, 1988; Jahr & Stevens, 1990*a*) as well as in the present study places the apparent blocking site almost entirely across the transmembrane electric field. Our results demonstrate that the narrow constriction represents a critical blocking site for extracellular Mg^{2+}, yet recent studies examining the block by impermeant organic cations suggest that it is positioned about 0·5–0·6 of the way across the electric field (Villarroel *et al.* 1995; Zarei & Dani, 1995). Since the adjacent NR2A-subunit asparagines form an apparent barrier for Mg^{2+} influx, it is unlikely that in terms of simple block Mg^{2+} penetrates any deeper into the channel than to the narrow constriction. Hence, following a simple Woodhull model, Mg^{2+} occupying its blocking site at the narrow constriction underlies a major part of the strong voltage dependence, perhaps about 0·5–0·6 of the 0·82 fractional electric distance.

Substitutions of the adjacent asparagines in the NR2A-subunit strongly attenuated the voltage dependence of the block. Over intermediate potentials (~−40 to −10 mV), this effect is apparently not due to changes in permeation (Fig. 12). The strongest attenuation occurred when Q (0·57) was substituted at NR2A(N0) or when G (0·50), S (0·53) or Q (0·46) was substituted at NR2A(N + 1). Surprisingly, these values converge around 0·5–0·6, a value similar to the position of the narrow constriction. Assuming that the position of the narrow constriction in the transmembrane electric field is unchanged by the substitutions, this result suggests that much of the additional voltage dependence is an intrinsic property of the NR2A amino acid residues at the narrow constriction. This conclusion is consistent with the results of Zarei & Dani (1994) who found that the NMDA receptor channel has a single file pore suggesting

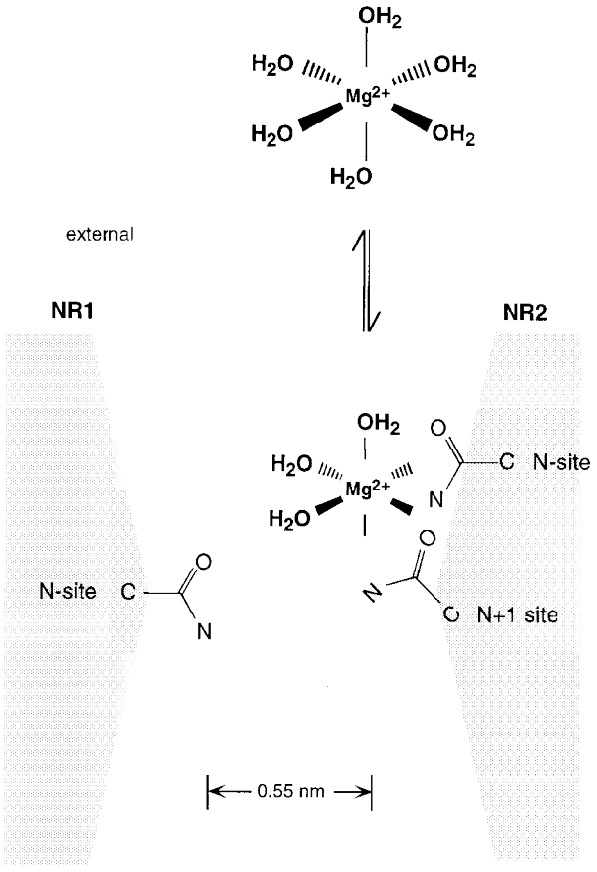

Figure 13. The adjacent asparagines in the NR2A-subunit underlie the block of NMDA receptor channels by extracellular Mg^{2+}

Schematic drawing of amino acid residues positioned at or near the narrow constriction. Mg^{2+} prefers an octahedral (sixfold) co-ordination. In solution, the co-ordination spheres are occupied by water. In the pore, bound Mg^{2+} loses anywhere from 1 to 6 waters of hydration with the free electron pairs in the carbonyl oxygen and/or amide nitrogen of the asparagine side chain substituting for the water molecules. The effective diameter of hydrated Mg^{2+}, which is not drawn to scale, is at least 0·7 nm considering only the primary hydration shell and assigning a diameter of 0·28 nm to a water molecule and 0·13 nm to Mg^{2+} (Frausto da Silva & Williams, 1991).

that the strong voltage dependence does not arise by multi-ion occupancy. Apparently, although other sites may contribute to the entry and exit of extracellular Mg^{2+} to its blocking site at the narrow constriction, when Mg^{2+} occupies this deep site, no other sites in the channel are occupied. How is the additional voltage dependence generated at the narrow constriction? Two alternative explanations can be considered. First, the strong voltage dependence of the block has been suggested to arise by ion–ion interactions within the pore (Zarei & Dani, 1995), and either of the adjacent asparagines could represent the 'permeant-ion' site proposed by these authors. Alternatively, the entire M2 segment or parts of it could move in the electric field as a function of voltage, with the bound Mg^{2+} acting as the voltage sensor. In this view, changes in binding of Mg^{2+} to the adjacent NR2A-subunit asparagines would reduce the dwell time of Mg^{2+} making it less sensitive to the transmembrane electric field and correspondingly reducing the voltage dependence of the block.

Contribution of the N-site asparagine in the NR1-subunit to extracellular Mg^{2+} block

The NR1-subunit N-site asparagine, which is critical for Ca^{2+} permeation (Burnashev *et al.* 1992), appears to make only a weak contribution to the block by extracellular Mg^{2+}. In all NR1(N0) mutant channels, the block by Mg^{2+} was strongly voltage dependent over intermediate potentials having δ values ranging from 0·80 (N0S) to 0·88 (N0Q), values that are very similar to those of wild-type (Table 2). However, the extent of block in these channels, compared with wild-type, was enhanced over intermediate potentials as seen by the higher voltage-independent affinity. Given that this effect occurred to an equivalent extent for the non-polar glycine and the polar serine and glutamine, all NR1(N0) substitutions may reflect to some extent a change in a general property of the channel. Indeed, when NR1(N0Q) is co-expressed with NR2A(N0Q), the resulting channels have multiple conductance levels, one of which has a higher affinity for Mg^{2+} than wild-type (Premkumar & Auerbach, 1996). This high-affinity site is weakly voltage dependent and presumably arises, at least in part, from the NR1(N0Q) substitution since NR1–NR2A(N0Q) channels do not display such behaviour (Sharma & Stevens, 1996). The net effect of multiple conductance levels with differential affinities for Mg^{2+} at the macroscopic level therefore appears to be an enhanced affinity with no change in the voltage dependence at least over intermediate potentials. At extreme potentials, more complex block patterns may arise.

Surprisingly, the substitution of a negative charge at NR1(N0) caused the strongest increase in the extent of Mg^{2+} block of all substitutions tested. Based on the available structural information, which places the NR1(N0) near the adjacent NR2A-subunit asparagines (Fig. 1*B*), this enhanced block could arise via an electrostatic mechanism and/or by offering Mg^{2+} an additional ligand. In summary, NR1(N0) substitutions do alter, albeit weakly, the block but the essential elements of the interaction between Mg^{2+} and the channel remain intact.

Conclusion

The amino acid residues forming the narrow constriction as contributed by the NR2-subunit in NMDA receptor channels represent a critical blocking site for extracellular Mg^{2+}. The results do not define how the strong voltage dependence of the block arises but suggest that much of the voltage dependence of the block is an intrinsic, local property of NR2-subunits at the narrow constriction.

Ascher, P. & Nowak, L. (1988). The role of divalent cations in the *N*-methyl-D-aspartate responses of mouse central neurones in culture. *Journal of Physiology* **399**, 247–266.

Bliss, T. V. P. & Collingridge, G. L. (1993). A synaptic model of memory: long-term potentiation in the hippocampus. *Nature* **361**, 31–39.

Burnashev, N., Schoepfer, R., Monyer, H., Ruppersberg, J. P., Günther, W., Seeburg, P. H. & Sakmann, B. (1992). Control by asparagine residues of calcium permeability and magnesium blockade in the NMDA receptor. *Science* **257**, 1415–1419.

DiFrancesco, D. (1982). Block and activation of the pacemaker channel in calf purkinje fibres: effects of potassium, caesium and rubidium. *Journal of Physiology* **329**, 485–507.

Falke, J. J., Drake, S. K., Hazard, A. L. & Peersen, O. B. (1994). Molecular tuning of ion binding to calcium signaling proteins. *Quarterly Reviews of Biophysics* **27**, 219–290.

Frausto da Silva, J. J. R. & Williams, R. J. P. (1991). *The Biological Chemistry of the Elements*, 1st edn. Clarendon Press, Oxford.

French, R. J. & Shoukimas, J. J. (1985). An ion's view of the potassium channel. *Journal of General Physiology* **85**, 669–698.

Hille, B. (1992). *Ionic Channels of Excitable Membranes*, 2nd edn, Sinauer Associates, Inc., Sunderland, MA, USA.

Hollmann, M. & Heinemann, S. (1994). Cloned glutamate receptors. *Annual Review of Neuroscience* **17**, 31–108.

Iino, M., Ozawa, S. & Tsuzuki, K. (1990). Permeation of calcium through excitatory amino acid receptor channels in cultured rat hippocampal neurones. *Journal of Physiology* **424**, 151–165.

Jahr, C. E. & Stevens, C. F. (1990*a*). A quantitative description of NMDA receptor–channel kinetic behavior. *Journal of Neuroscience* **10**, 1830–1837.

Jahr, C. E. & Stevens, C. F. (1990*b*). Voltage dependence of NMDA-activated macroscopic conductances predicted by single-channel kinetics. *Journal of Neuroscience* **10**, 3178–3182.

Johnson, J. W. & Ascher, P. (1990). Voltage-dependent block by intracellular Mg^{2+} of *N*-methyl-D-aspartate channels. *Biophysical Journal* **57**, 1085–1090.

Kuner, T., Wollmuth, L. P., Karlin, A., Seeburg, P. H. & Sakmann, B. (1996). Structure of the NMDA receptor channel M2 segment inferred from the accessibility of substituted cysteines. *Neuron* **17**, 343–352.

Li-Smerin, Y. & Johnson, J. W. (1996). Kinetics of the block by intracellular Mg^{2+} of the NMDA-activated channel in cultured rat neurons. *Journal of Physiology* **491**, 121–135.

MacDermott, A. B., Mayer, M. L., Westbrook, G. L., Smith, S. J. & Barker, J. L. (1986). NMDA receptor activation increases cytoplasmic calcium concentration in cultured spinal cord neurones. *Nature* **321**, 261–263.

Mayer, M. L. & Miller, R. J. (1988). Excitatory amino acid receptors, second messengers and regulation of intracellular Ca^{2+} in mammalian neurons. *Trends in Pharmacological Sciences* **11**, 254–260.

Mayer, M. L. & Westbrook, G. L. (1987). Permeation and block of *N*-methyl-D-aspartic acid receptor channels by divalent cations in mouse cultured central neurones. *Journal of Physiology* **394**, 501–527.

Mayer, M. S., Westbrook, G. L. & Guthrie, P. B. (1984). Voltage-dependent block by Mg^{2+} of NMDA responses in spinal cord neurones. *Nature* **309**, 261–263.

Moisescu, D. G. & Thieleczek, R. (1978). Calcium and strontium concentration changes within skinned muscle preparations following a change in the external bathing solution. *Journal of Physiology* **275**, 241–262.

Mori, H., Masaki, H., Yamakura, T. & Mishina, M. (1992). Identification by mutagenesis of a Mg^{2+}-block site of the NMDA receptor channel. *Nature* **358**, 673–675.

Nowak, L., Bregestovsky, P., Ascher, P., Herbet, A. & Prochiantz, A. (1984). Magnesium gates glutamate-activated channels in mouse central neurones. *Nature* **307**, 462–465.

Nowak, L. M. & Wright, J. M. (1992). Slow voltage-dependent changes in channel open-state probability underlie hysteresis of NMDA responses in Mg^{2+}-free solutions. *Neuron* **8**, 181–187.

Premkumar, L. S. & Auerbach, A. (1996). Identification of a high affinity divalent cation binding site near the entrance of the NMDA receptor channel. *Neuron* **16**, 869–880.

Ruppersberg, J. P., von Kitzing, E. & Schoepfer, R. (1994). The mechanism of magnesium block of NMDA receptors. *Seminars in the Neurosciences* **6**, 87–96.

Sakurada, K., Masu, M. & Nakanishi, S. (1993). Alteration of Ca^{2+} permeability and sensitivity to Mg^{2+} and channel blockers by a single amino acid substitution in the *N*-methyl-D-aspartate receptor. *Journal of Biological Chemistry* **268**, 410–415.

Schneggenburger, R. & Ascher, P. (1997). Coupling of permeation and gating in an NMDA-channel pore mutant. *Neuron* **18**, 167–177.

Sharma, G. & Stevens, C. F. (1996). A mutation that alters magnesium block of *N*-methyl-D-aspartate receptor channels. *Proceedings of the National Academy of Sciences of the USA* **93**, 9259–9263.

Sheng, M., Cummings, J., Roldan, L. A., Jan, Y. N. & Jan, L. Y. (1994). Changing subunit composition of heteromeric NMDA receptors during development of rat cortex. *Nature* **368**, 144–147.

Stephenson, D. G. & Thieleczek, R. (1986). Activation of the contractile apparatus of skinned fibres of frog by the divalent cations barium, cadmium and nickel. *Journal of Physiology* **380**, 75–92.

Stout, A. K., Li-Smerin, Y., Johnson, J. W. & Reynolds, I. J. (1996). Mechanisms of glutamate-stimulated Mg^{2+} influx and subsequent Mg^{2+} efflux in rat forebrain neurones in culture. *Journal of Physiology* **492**, 641–657.

Villarroel, A., Burnashev, N. & Sakmann, B. (1995). Dimensions of the narrow portion of a recombinant NMDA receptor channel. *Biophysical Journal* **68**, 866–875.

Wollmuth, L. P., Kuner, T. & Sakmann, B. (1998). Intracellular Mg^{2+} interacts with structural determinants of the narrow constriction contributed by the NR1-subunit in the NMDA receptor channel. *Journal of Physiology* **506**, 33–52.

Wollmuth, L. P., Kuner, T., Seeburg, P. H. & Sakmann, B. (1996). Differential contribution of the NR1- and NR2A-subunits to the selectivity filter of recombinant NMDA receptor channels. *Journal of Physiology* **491**, 779–797.

Woodhull, A. M. (1973). Ionic blockage of sodium channels in nerve. *Journal of General Physiology* **61**, 687–708.

Zarei, M. M. & Dani, J. A. (1994). Ionic permeability characteristics of the *N*-methyl-D-aspartate receptor channel. *Journal of General Physiology* **103**, 231–248.

Zarei, M. M. & Dani, J. A. (1995). Structural basis for explaining open-channel blockade of the NMDA receptor. *Journal of Neuroscience* **15**, 1446–1454.

Acknowledgements

We thank Peter H. Seeburg for his generous support, Drs C. Beck, N. Burnashev, D. Feldmeyer, J. Mosbacher and A. Villarroel for their comments on the manuscript, H. Spiegel for expert secretarial assistance, and M. Kaiser and S. Grünewald for technical assistance. This work was supported in part by a long-term Human Frontier Science Fellowship (L.P.W.).

Corresponding author

L. P. Wollmuth: Abteilung Zellphysiologie, Max-Planck-Institut für medizinische Forschung, Jahnstrasse 29, D-69120 Heidelberg, Germany.

Email: wollmuth@sunny.mpimf-Heidelberg.mpg.de